Sustainable Structures
ISSN: 2789-3111 (Print); ISSN: 2789-312X (Online)
http://www.sustain-dpl.com/journal/sust
DOI: 10.54113/j.sust.2026.000119

ORIGINAL ARTICLE

Sustainable architectural top additions with light-frame timber structures also incorporating dissipative braces

Arianna Straulino[a,*], Stefano Sorace[a] , Naisa Hoxha[a], Gloria Terenzi[b]

[a]Polytechnic Department of Engineering and Architecture, University of Udine, Via delle Scienze 206, 33100 Udine, Italy
[b]Department of Civil and Environmental Engineering, University of Florence, Via Santa Marta 3, 50139 Florence, Italy
[*]Corresponding Author: Arianna Straulino. Email: arianna.straulino@uniud.it

Abstract: A study on sustainable architectural top additions for reinforced concrete (RC) buildings based on the use of light-frame timber (LFT) structures is presented in this article. The objectives of the study are: a) to evaluate the possibilities offered by traditional LFT solutions; b) to propose a new LFT configuration that incorporates a small-sized dissipative bracing (DB) system, easily hidden behind the sheathing panels of the timber structure; c) to extend the installation of the DB system to a small number of perimeter spans of the underlying RC structure in order to achieve its seismic retrofit with no architectural intrusion and interruption in the use of the building. For the simulated application of these structural solutions, a representative real case study is selected, consisting of a two-storey RC residential building characterized by an eccentric position of the RC core surrounding the stairwell. This causes significant seismic torsional response effects in plan, making this case particularly challenging. A single-storey architectural top addition is designed for the building, covering 63% of the flat roof level. The results of the study show that: thanks to its intrinsic lightness, the traditional LFT structure produces a moderate increase in inter-storey drifts and stress states in the structural members of the underlying RC structure, as compared to as-built conditions; the incorporation of the DB system in only eight spans of the LFT structure in the longitudinal direction of the building, and four spans in the transversal direction, allows to meet the basic design objective of almost completely annulling the increase in seismic demand caused by the construction of the upper addition; the seismic retrofit of the RC structure is achieved by extending the installation of the DB system only to 8% of its transversal spans, situated on the side façade, and no longitudinal spans, without any architectural impact on the building.

Keywords: light-frame timber structures, top additions, dissipative braces, pressurized fluid viscous dampers, seismic retrofit

1 Introduction

Building top additions constructed with light-frame timber (LFT) structural solutions are attracting growing interest from academia and professionals, as well as from companies, due to their considerable potential in terms of architectural, structural and environmental sustainability, and economic benefits. Indeed, they offer several advantages, including: very high environmental compatibility of wood; greater intrinsic lightness of wooden structures as compared, for the same structural performance, to solutions made with other structural materials, resulting in a reduction in additional mass, which is

Received: 4 April 2026; Received in revised form: 12 June 2026; Accepted: 12 July 2026

particularly important for interventions in seismic zones; flexibility and speed of installation (with elements being either assembled on site or wholly prefabricated); an equally simple possibility of future dismantling and recycling, or adaptation to new functional and usage needs, which is an essential requirement from the point of view of sustainability in the construction sector; aesthetic appeal; versatility of finishes and integration with thermal insulation and energy efficiency improvement interventions, etc.

For a long time, the construction of LFT structures has been based on the traditional platform frame technique. Since the beginning of 1990s, some proposals have been formulated to incorporate supplemental damping systems into LFT shear walls in seismic areas, so as to prevent or limit their damage, and improve their resilience [1]. The first studies considered friction dampers inserted at the corners of the walls [2]. Viscoelastic dampers were adopted in [3], examining some different installation layouts, the most efficient of which proved to be a single diagonal bracing configuration. Tension yielding steel bars were proposed as special damping elements in [4], and self-centering steel cables were incorporated to reduce residual deformations after seismic events in [5]. Fluid viscous dampers were analysed in single bracing diagonal layout in [6], or placing them horizontally at the base of chevron-shaped braces in [7]. In order to amplify lateral displacements, with the aim of exploiting the damping capacity of fluid viscous devices better, a toggle brace configuration was adopted in [8], borrowing it from previous applications to reinforced concrete (RC) structures. This solution was extended to a highly vulnerable structural layout, represented by soft-storey wood-frame buildings [9]-[12], not strictly connected to classical LFT platform frame structures. The latter were investigated further in [13], by inserting steel braced frames in some spans of the structure and connecting them to the LFT panels by means of steel collectors, with interposed metallic yielding hysteretic dissipaters. Recently, studies have focused on the energy dissipation mechanisms associated with the response of sheathing panels [14], hold-down brackets [15] and nails connecting the sheathing panels to the frame elements [16][17].

Over the last decade, the application of supplemental damping systems has focused primarily on heavy-frame timber structures, as well as on cross-laminated shear-wall and other types of shear-wall timber buildings. Friction, metallic yielding and fluid viscous dampers have been considered for installation also in these structures. Furthermore, new special energy dissipation mechanisms, based on rocking or post-tensioning principles, have been specifically proposed for them. The reason why there has been no further increase in interest in the application of dissipative systems to LFT structures mainly lies in the fact that their sheathing panels provide a relatively high racking stiffness. This constrains lateral displacements even in the presence of significant seismic damage to studs and plates, their mutual joints and the connections to the panels, and the hold-down brackets. Consequently, dissipators achieve relatively small displacements even when amplifying installation layouts are adopted, such as the toggle brace for fluid viscous devices mentioned above. This considerably limits their damping action, as well as the associated benefits on the response of LFT structures. At the same time, for architectural and functional reasons, it is necessary to use only small-sized dampers and supporting elements, so that they can fit within the internal thickness of the LFT panels.

Based on these considerations, it seemed of interest to re-examine the possibility of incorporating dissipative technologies into LFT structures, thereby offering new contributions to the research carried out in previous decades. Furthermore, given the growing interest in roof extensions constructed using LFT panels, the study presented in this article is focused on the incorporation of dissipative bracing (DB) systems specifically into LFT-based top additions. Indeed, for these applications, the advantages lie both in the advanced protection of the LFT structures and in limiting the increase in seismic response caused in the underlying buildings by the construction of the extra-storeys.

In line with the research conducted by the second and fourth authors over the past 25 years, pressurized fluid viscous (PFV) spring-dampers were selected as the dissipative devices to be installed in the LFT panels. The choice was motivated by the fact that, on one hand, the extremely high specific damping capacity of this class of devices produces a significant energy dissipation effect even for very small displacements; on the other hand, the compact size of the PFV spring-dampers and their supporting steel trusses allows them to be easily hidden behind the OSB (Oriented Strand Board) cladding panels of the LFT structure.

The study presented in this article, developed within the Italian national research programme "ReLUIS-DPC Project 2024-2026 – Work Package 12: Steel, timber and composite civil and industrial constructions", is particularly focused on the addition of LFT structures on top of RC frame buildings, with the aim of: a) evaluating the structural performance of traditional "platform-frame"-type LFT solutions, providing contributions in terms of design and finite element modelling, and assessing the consequences of such additions on the seismic response of the underlying structures; b) exploring the possibilities offered by the incorporation of a PFV-equipped DB system into the LFT panels, with the objective of substantially limiting the increase in seismic demand on the building caused by the upper addition; c) extending the installation of the DB system to a selected number of perimeter spans of the underlying RC structure in order to achieve its seismic retrofit with no architectural intrusion or interruption in the use of the building, thus emphasizing the overall sustainability of this intervention strategy.

A real building was selected as a case study for the simulated application of the three structural solutions, since the complexity of a real-world building always allows for a more in-depth examination of all aspects related to the application of a structural system and a special technology, as compared to purely numerical simple structural models. The building is a two-storey RC residential block designed in the 1990s, when the Italian municipality in which it is located was classified as a non-seismic zone. Subsequently, the new classification of the Italian territory provided for by the 2008 edition of the national Technical Standards placed the municipality in a moderate seismic zone, confirmed by the 2018 update of the Standards. The building is characterized by an eccentric position of the RC core surrounding the stairwell. This layout causes a notable irregularity in plan and thus significant torsional seismic response effects, making this case study particularly challenging for all three structural interventions. The top addition planned in the architectural design covers 63% of the flat roof level.

The following Sections report: the seismic assessment analysis of the building in its current conditions; the modelling criteria and design of the LFT superstructure in the traditional configuration and in the presence of the PFV-equipped DB system; comparisons between the seismic performance of the top addition and the entire building for the two different solutions; the design and performance evaluation of the retrofit intervention based on the incorporation of the DB technology also in some spans of the existing structure; notes on the architectural impact, sustainability and costs of the three interventions.

2 Geometrical and structural characteristics of case study building

The plan dimensions of case study building are 36.3 m × 22.2 m, with a surface area of 806 m^2. The ground and first storey heights are 3.4 m and 3.15 m, resulting in a total height above ground of 6.55 m. The height of the RC core is equal to 10.35 m. **Fig. 1** shows the structural plan of the ground storey, including the *X* and *Y* axes of the Cartesian reference system assumed in the finite element analyses (being *Z* the vertical axis), and a longitudinal and a transversal section.

The structure of the first and roof floors is 280 mm thick and made of 240 mm-high partly prefabricated RC joists, parallel to *Y*, clay lug bricks, and a 40 mm thick upper RC slab. The beams in longitudinal direction, parallel to *X*, have an in-depth cross section of 1000 mm × 280 mm in the four internal alignments, and 350 mm × 280 mm in the two perimeter alignments. All beams in transversal direction have in-depth section of 400 mm × 280 mm, except for the one facing the "C-shaped" RC core enclosing the stairwell (C-3/C-4 span), sized 1000 mm × 280 mm, and those belonging to the A alignment, with section of 300 mm × 280 mm. The 200 mm thick RC core has dimensions of 5555 mm along *X* and 3000 mm along *Y*. All columns have rectangular section with the larger side parallel to *Y*, equal to 600 mm on the ground storey, except for columns located on A-2, A-3, A-4 and A-5 fixed lines (**Fig. 1**), whose side is 400 mm long. On the first storey, the *Y*-parallel side is 600 mm long, for all columns belonging to the perimeter longitudinal alignments (1 and 6), and 400 mm long, in the four internal alignments (2 through 5). The *X*-parallel side is equal to 200 mm for all columns on both storeys. On the ground storey, the distance between the columns is equal to 6 m in the internal longitudinal alignments, and 3 m in the external ones. Columns located on B-1, E-1, H-1 and M-1 fixed lines on the south façade, and C-6, F-6, I-6 and N-6 fixed lines on the north façade do not continue on the first storey. In transversal direction, the distance between the columns is equal to 3.6 m for the four lateral spans and 6.8 m for the central span.

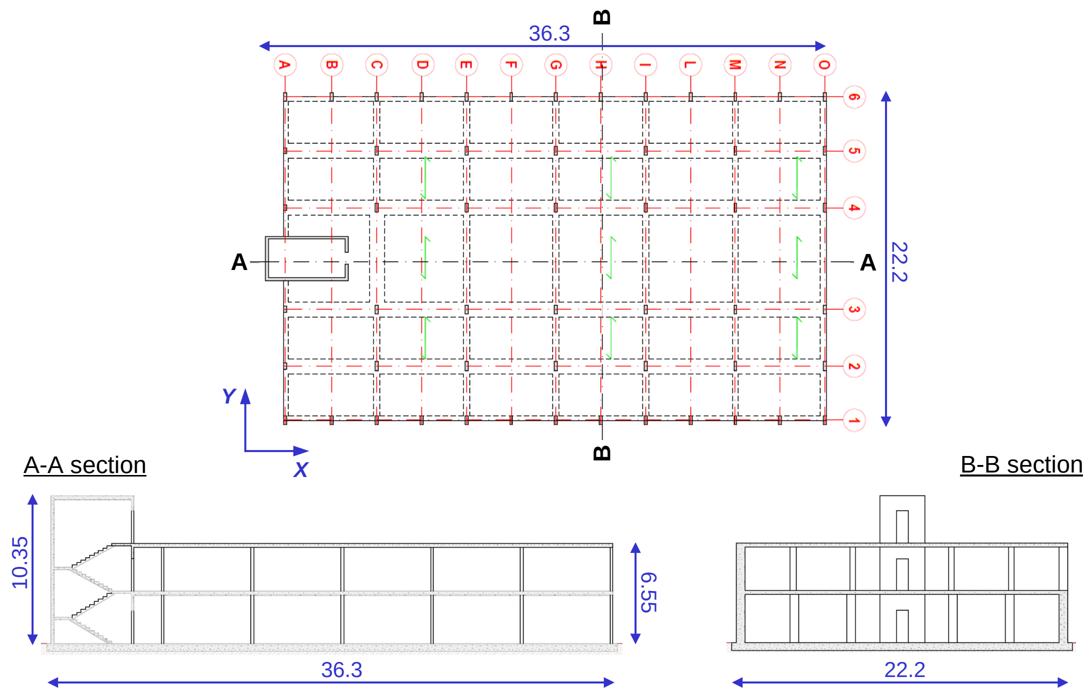

Fig. 1. Ground storey structural plan, longitudinal and transversal sections of case study building in current state (dimensions in meters)

The foundation is constituted by a continuous 500 mm-thick RC slab, incorporating a mesh of 1500 mm-wide in-depth rib beams plotted under the longitudinal and transversal frame alignments and the C-shaped core. This solution, oversized in terms of stress states transferred to the underlying soil, was adopted in the original design of the building to protect the ground storey from the seasonal variations of water table level. This allows to design the top addition of the building with no need to enlarge the foundation slab or introduce piles under possible critical zones. Two 3D-reconstructed architectural views of the building in its current conditions are shown in **Fig. 2**.

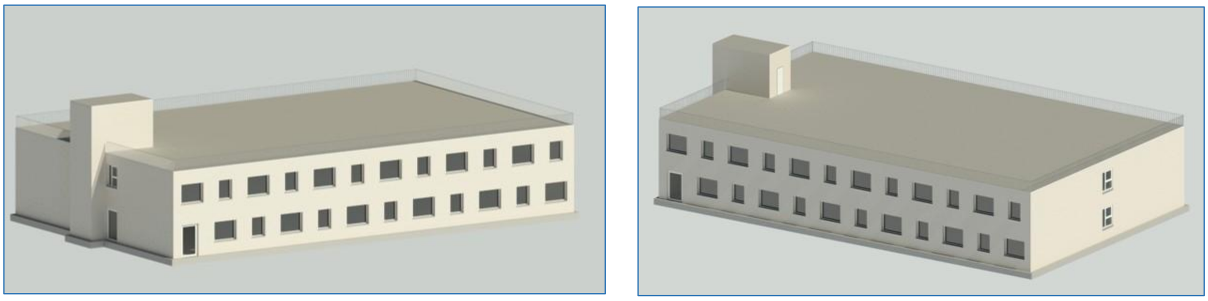

Fig. 2. 3D architectural views of case study building in current state.

3 Seismic assessment analysis in current state

The seismic assessment study of the building was carried out, via time-history linear analysis, by using the finite element model of the structure displayed in **Fig. 3**, generated with SAP2000NL calculus program [18]. Frame-type elements were assumed for columns and beams, and shell elements for the stairwell core.

The analyses were performed for the Serviceability Design Earthquake (SDE, with 63% probability of being exceeded over the reference time-period, V_R) and the Basic Design Earthquake (BDE, with 10%/V_R probability) hazard levels assumed by the current Italian Standards [19]. The V_R period was fixed at 50 years, obtained by multiplying the nominal structural life V_N of 50 years by a coefficient of use C_u equal to 1, corresponding to the residential use of the building. A set of seven groups of three accelerograms each was applied as input to the time-history analyses.

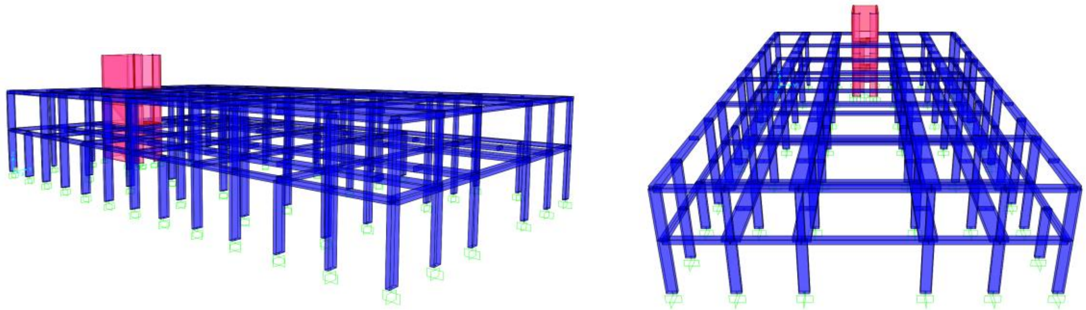

Fig. 3. Views of the finite element model of the structure in current state.

The artificial ground motions were generated, using the opensource software SIMQKE_GR [20], from the elastic pseudo-acceleration response spectra, at linear viscous damping ratio of 0.05, assumed for the municipality where the building is located, drawn in **Fig. 4**.

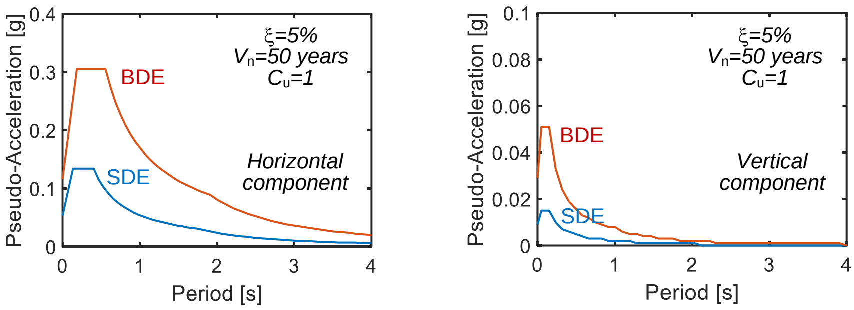

Fig. 4. Horizontal and vertical SDE and BDE-scaled pseudo-acceleration elastic response spectra.

Starting from these spectra, the software creates horizontal and vertical ground motions, checking their spectral compatibility. In detail, according to [19], the mean value of the ordinate of the spectrum of each accelerogram must be greater than 90% of the target response spectrum value. Furthermore, according to the prescriptions of [19], the duration of each ground motion was set to 30 seconds, including a 10 second-long pseudo-stationary branch. In the analyses, for each group of input motions, one accelerogram was applied in *X* direction, one in *Y* and one in *Z*.

A modal analysis of the structure was initially carried out, which shows a first mode, mixed translational along *Y*–rotational around *Z*, with vibration period of 0.568 s and effective modal mass (EMM) equal to 57.1% of the total seismic mass of the building along *Y* and 24.8% around *Z*, and a first translational mode along *X*, with period of 0.218 s and EMM of 81.1%. A total of 4 modes is needed to activate a summed modal mass (SMM) greater than 85% both in *Y* and *X*, and 3 modes in *Z*, as the rotational modes are associated to the translational modes in *X* and *Y*. Although designed with no reference to Seismic Standards, the reinforcement details of the structural members are not poor for stirrups and ties, with well-anchored 135-degree hooks in all columns and beams of the elevation structure and the foundation rib beams, as well as for longitudinal bars and electro-welded steel nets, with appropriate lap splices. In addition, the 1996 edition of the Italian Standards of RC structures, according to which the building was designed, imposed minimum percentages of reinforcement in flexure and shear similar to the ones requested for structures located in low seismicity zones at the time. In view of this, and by considering the irregularity of the building in plan, according to the suggestions of the Instructions for the application of the current Italian Standards [21] a behaviour factor *q* equal to 2 was assumed in the stress state checks in flexure and compression-flexure (corresponding to moderately ductile mechanisms), and 1.5 in shear (brittle mechanisms). Based on the assumptions recapitulated above, the results of the time-history analyses at the SDE highlight that: (a) all structural members meet stress state checks; (b) the maximum values of the interstorey drift ratio, *IDR* (i.e. the ratio of the interstorey drift to the interstorey height), always attained on the first storey, are equal to 0.1% in the stiffer direction *X* (reached in alignment 1 in plan) and 0.4% in *Y* (alignment O). The latter value is below the *IDR* limit of 0.5% fixed by the Italian Standards as basic requirement for the attainment of the Immediate Occupancy (IO) seismic performance level for infilled frame buildings, like the case study one.

At the BDE, 35% of columns are in unsafe conditions in compression-biaxial flexure and 20% of beams in flexure, on the ground storey, and 15% of columns and 18% of beams on the first storey, respectively. These members are identified with red (columns) and blue (beams) lines in the schematic views of the structure displayed in **Fig. 5**. As expected, they are mainly located opposite in plan to the RC core. Furthermore, no beam parallel to X is in unsafe conditions.

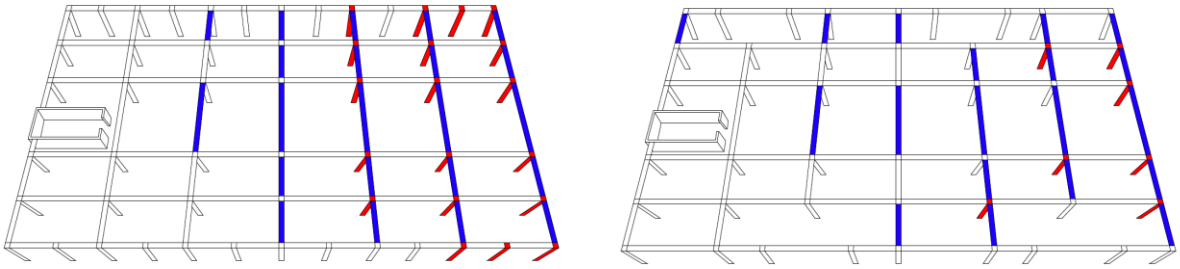

Fig. 5. Location of the structural elements in unsafe conditions in current state (left: ground storey, right: first storey).

By way of example of the response at this hazard level, the M_Y–M_X biaxial moment interaction curves (being M_Y, M_X the bending moments around Y and X axes) obtained from the most demanding among the seven groups of accelerograms, are plotted in **Fig. 6** for the most stressed columns with section 200 mm × 600 mm, located on the ground storey O-1 fixed line, and 200 mm × 400 mm, located on the first storey O-2 fixed line. The borders of the safe domains, traced out for comparison in **Fig. 6**, are exceeded by about 37% and 28% for columns O-1 and O-2, respectively.

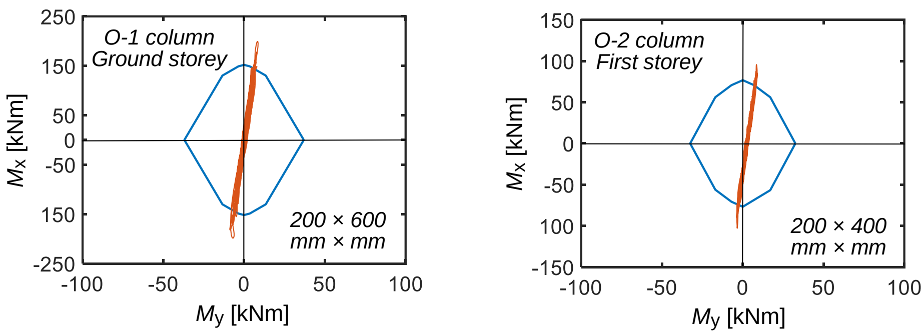

Fig. 6. M_y-M_x biaxial moment interaction curves for ground storey O-1 column and first storey O-2 column obtained from the most demanding BDE-scaled group of accelerograms (orange), and relevant biaxial moment safe domains (blue).

It is noted that the significant contribution of the rotational component around Z to the modal response of the structure is confirmed by the results of the time-history analyses. Indeed, drifts increase almost linearly along Y, from the A alignment in plan adjacent to the RC core (with *IDR* values at the BDE equal to 0.1% on the ground storey and 0.14% on the first storey) to the O alignment located on the opposite side (0.65%—ground storey, 1.19%—first storey). Similar to the above-mentioned values referred to the SDE, the *IDRs* in X are about four times smaller than in Y also at the BDE, and are not affected by the torsional response component, consistently with the purely translational first mode along X. In light of this, in the following Sections, dedicated to the three different interventions on the building, the *IDR* response is discussed only for the transversal alignment O, which is subject to the largest seismic response displacements. The *IDR* peak value of 1.19% on the first storey along O corresponds to possible collapse conditions of relevant infills [22] (with values of about 0.8% and 1% in the I and M alignments denoting very severe and irreparable damage conditions, respectively). The peak *IDR* value of 0.65% achieved on the ground storey assesses severe but still repairable damage.

4 Light-frame timber top addition

4.1 Design and modelling of the LFT structure

As displayed by the top storey plan and the cross sections in **Fig. 7**, the 3.8 m high upper addition extends across the three central transverse spans of the building. The two side spans are not covered, to serve as terraces for the apartments of the new storey. The surface area of the addition is 508 m^2, equal to 63% of the plan of the building. General views of the LFT bare structure are drawn in **Fig. 8** over the 3D architectural model of the building, shown in **Fig. 2** in its current state. The LFT members are made of C24-strength class coniferous timber, according to the classification of CNR-DT 206-R1 Instructions for design, execution and control of timber structures [23], with characteristic bending, compressive and tensile strengths of 24 MPa, 21 MPa and 14.5 MPa, respectively.

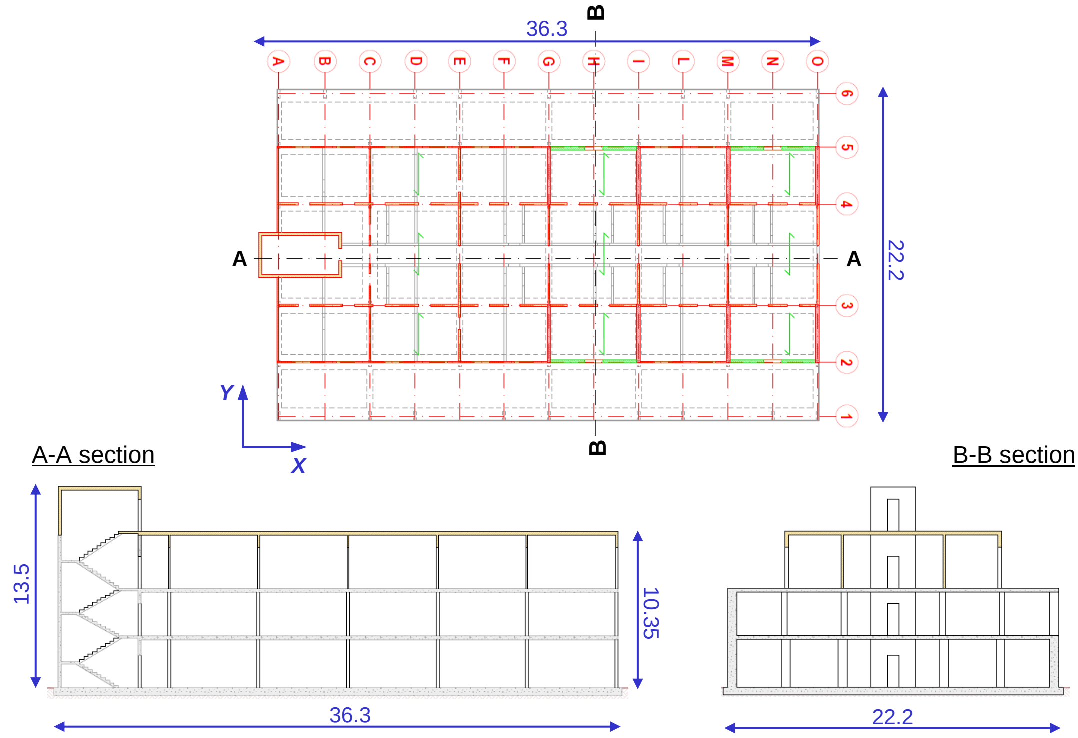

Fig. 7. Top storey structural plan, and longitudinal and transversal cross sections including the LFT top addition (dimensions in meters)

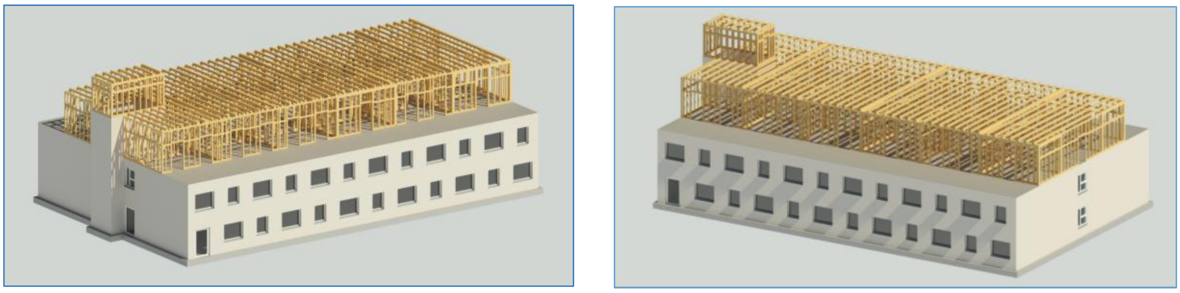

Fig. 8. 3D architectural views of case study building including the LFT top addition before installing the OSB sheathing panels.

The LFT frames are sheathed on both sides by 15 mm-thick OSB panels nailed to the studs, as well as to the bottom, intermediate blocking and top plates of the frames. Studs are sized 80 mm (side parallel to the frame plan) ×120 mm (transversal side) and all plates 120 mm × 120 mm, for the frames situated along the transversal and external longitudinal alignments in plan. Studs are sized 80 mm × 150 mm, top and bottom plates 150 mm × 150 mm and blocking plates 120 mm × 150 mm, in the internal longitudinal alignments and the top extension of the stairwell core. The panels are connected to the underlying beams of the RC structure by means of special commercial continuous aluminium profiles [24], instead of traditional sets of angle brackets. These profiles, which eliminate any contact between the bottom plate of panels and the concrete surface of beams, ensuring protection from capillary rising damp and high durability, are connected to the panels by a close series of high bond nails with a diameter of 4 mm, and fastened to the RC beams by means of steel expansion anchors. Additional hold-down stiffened angle brackets are nailed to the two end studs. Drawings of a frame panel are shown in **Fig. 9**, referred to the panels belonging to the transversal and external longitudinal alignments (the remaining panels are identical, except for the width of studs and top and bottom plates, equal to 150 mm instead of 120 mm, as mentioned above).

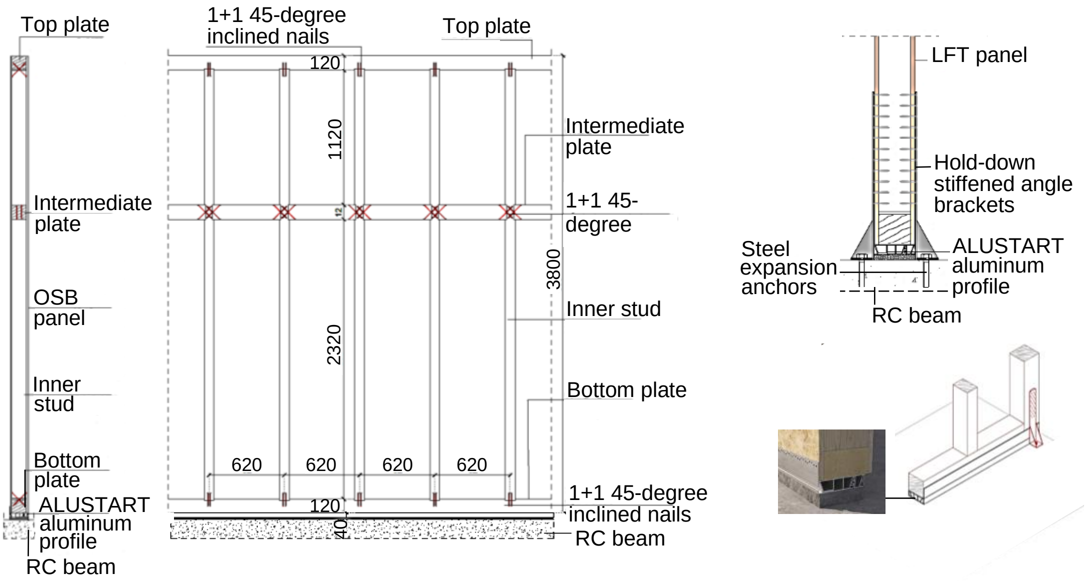

Fig. 9. Details of a LFT panel and the connections to the underlying RC beam (dimensions in millimeters)

The structure of the flat roof is made of C24 class beams parallel to Y, with sections of 160 mm × 180 mm in the two lateral spans and 260 mm × 260 mm in the central span, 25 mm-thick roof boards, and 25 mm-thick upper OSB sheathing panels. The beams are connected at both ends by pairs of inclined screws with a diameter of 6 mm.

Views of the finite element model of the structure in the presence of the superelevation are shown in **Fig. 10**. As visualized by these images, the LFT structure was simulated by using equivalent shell-type finite elements with orthotropic mechanical behaviour, made of homogeneous material. The Young modulus, E, shear modulus, G, and mass density, ρ, of the latter were calibrated by using the equivalence criteria formulated in [25], reassessed in [26] and [27], and revised in this study for the specific types of connectors used in the design of the top added structure, as summarized below.

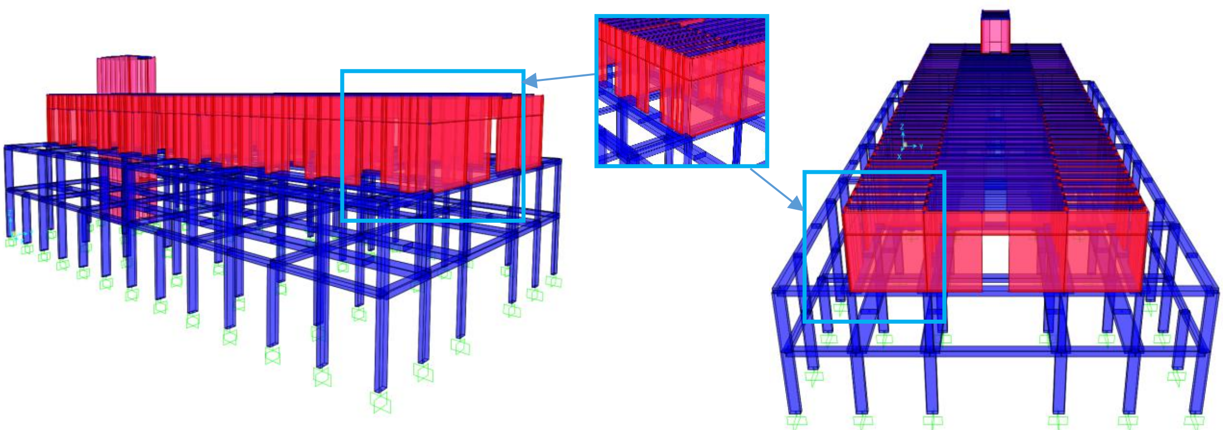

Fig. 10. Views of the finite element model of the structure including the LFT top addition.

The equivalent shear modulus of the material constituting the shell elements, G_{eq}, was computed by the expression of the elastic lateral shear stiffness of the LFT panel, coinciding with the racking stiffness in the hypothesis of neglecting the flexural deformability of the panel:

$$G_{\text{eq}} = \frac{1.2 \cdot h}{b \cdot L} \cdot K_{\text{eq}} \tag{1}$$

being h, L, b the height, base and total width (sum of the widths of the frame elements and the OSB sheets) of the panel, and K_{eq} its equivalent shear stiffness. K_{eq} is calculated as follows:

$$K_{\text{eq}} = \frac{1}{\frac{1}{K_{\text{OSB}}} + \frac{1}{K_{\text{n}}} + \frac{1}{K_{\text{anc}}} + \frac{1}{K_{\text{tb}}} + \frac{1}{K_{\text{bb}}}} \tag{2}$$

where the five terms at the denominator represent the stiffness contributions of: the OSB sheets (K_{OSB}); the perimeter nails of the OSB sheets (K_{n}); the bars (or expansion anchors) fastening the panel to the underlying RC beam (K_{anc}); the screws (or nails) connecting the panel to the top floor beams (K_{tb}); and the screws (or nails) connecting the panel to the aluminum profile placed at its bottom base (K_{bb}). Considering that both the design of the LFT structure and the finite element analyses were carried out in the elastic field, the stiffness contributions were computed by referring to the elastic response of the OSB sheets and the four types of connectors. Basic technical design formulas reported in Standards [19] and collected in [26], listed below, were used to calculate the five stiffness terms:

$$K_{\text{OSB}} = \frac{G_{\text{OSB}}^{\cdot m \cdot t \cdot L}}{1.2 \cdot h} \tag{3}$$

where G_{OSB} is the shear modulus of the OSB sheets, m is the number of sheet layers, t the single sheet thickness, and L and h are base and height of the panel;

$$K_{\text{n}} = \frac{L^{2 \cdot m\ 2 \cdot k_{\text{ser,n}}}}{1.2 \cdot h} \tag{4}$$

being: $N = m \cdot \left(\frac{2L}{i_{\text{n}}} + \frac{(2n+2)h}{i_{\text{n}}} \right)$ the total number of nails (without pre-drilling) put on the perimeter of each OSB panel (the internal nails, which only contribute to the stability of the OSB sheets, are omitted in this calculation), where n is the number of vertical joints, i_{n} the nail spacing, $k_{\text{ser,n}}$ the service stiffness of each nail, expressed as: $k_{\text{ser,n}} = \frac{\left(\sqrt{Q_{m\text{frame}} \cdot Q_{\text{m,OSB}}}\right)^{1.5} \cdot d_{\text{nail}}^{0.8}}{30}$, with $\rho_{\text{m,frame}}$, $\rho_{\text{m,OSB}}$ medium mass densities of the timber frame and the OSB panels, respectively, and d_{nail} the diameter of a nail;

$$K_{\text{anc}} = k_{\text{bar}} \frac{L}{i_{\text{b}}} \tag{5}$$

where $k_{\text{bar}} = 2 \cdot \frac{Q_{\text{mframe}}^{1.5} \cdot d_{\text{bar}}}{23}$ is the stiffness of the bars connecting the bottom timber plate to the RC beams, with d_{bar} the diameter of a bar, and i_{b} the mutual spacing of the bars;

$$K_{\text{tb}} = k_{\text{screw,t}} \frac{L}{i_{\text{screw,t}}} \tag{6}$$

$$K_{\text{bb}} = k_{\text{screw,b}} \frac{L}{i_{\text{screw,b}}} \tag{7}$$

where $k_{\text{screw,t}} = \dfrac{Q_{\text{mframe}}^{1.5} \cdot d_{\text{screw,t}}}{23}$, $k_{\text{screw,b}} = \dfrac{Q_{\text{mframe}}^{1.5} \cdot d_{\text{screw,b}}}{23}$ represent the stiffness of a screw connecting the panel to the top floor beams or to the aluminum base profile, $d_{\text{screw,t}}$, $d_{\text{screw,b}}$ the relevant diameters, and $i_{\text{screw,t}}$ and $i_{\text{screw,b}}$ the spacings of the screws on the top and base connections, respectively.

The equivalent Young modulus of the material constituting the shell elements, E_{eq}, and its equivalent mass density, ρ_{eq}, were calculated using a weighted average, based on the cross-sectional area, of both the Young modulus and mass densities of the engineered wood constituting the OSB sheets, E_{OSB}, ρ_{OSB}, and the solid wood of the frame members, E_{swf}, ρ_{swf}. Hence, named A_{OSB} the area of the base section of the two OSB sheets of a panel, A_{swf} the sum of the areas of the cross sections of its studs, and A_{nom} the nominal area of the base section of the panel, given by the product of its base and width, E_{eq}, ρ_{eq} are calculated as follows:

$$Q_{\text{eq}} = \frac{Q_{\text{OSB}} \cdot A_{\text{OSB}} + E_{\text{swf}} \cdot A_{\text{swf}}}{A_{\text{nom}}} \tag{8}$$

$$Q_{\text{eq}} = \frac{Q_{\text{OSB}} \cdot A_{\text{OSB}} + Q_{\text{swf}} \cdot A_{\text{swf}}}{A_{\text{nom}}} \tag{9}$$

4.2 Seismic assessment analysis with the added LFT structure

Like in current state, the modal analysis highlights a first mode, mixed translational along *Y*–rotational around Z, with vibration period of 0.697 s and EMM equal to 60.2% along *Y* and 21.1% around *Z*, and a first translational mode along *X*, with period of 0.275 s and EMM of 82.9%. Four modes are needed to activate a SMM greater than 85% in *Y*, 23 modes in *X*, and 5 in *Z*.

At the SDE, all structural members meet the stress state checks also in the presence of the top addition. At the BDE, the percentage of columns in unsafe conditions increases from 35% of current state to 41%, on the ground storey, and from 15% to 30%, on the first storey. The number of beams not meeting the stress state checks remains practically unchanged. Similarly to **Fig. 5** relating to current conditions, **Fig. 11** offers an overview of columns (red lines) and beams (blue lines) in unsafe conditions on the two storeys, highlighting the moderate differences caused by the construction of the LFT addition.

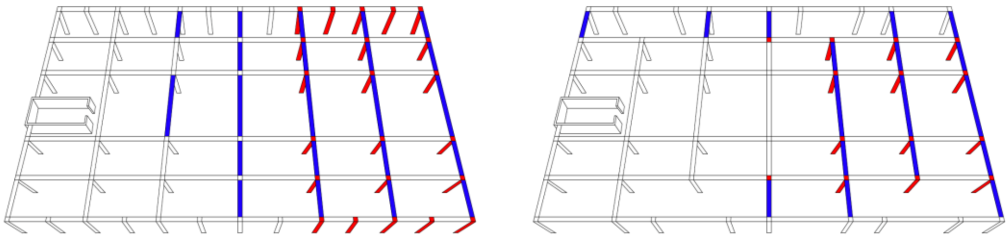

Fig. 11. Location of the structural elements in unsafe conditions in the presence of the LFT top addition (left: ground storey, right: first storey).

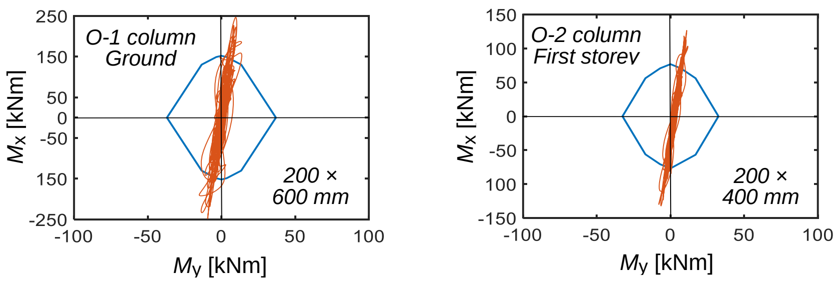

Fig. 12. M_y-M_x biaxial moment interaction curves for ground storey O-1 column and first storey O-2 column obtained from the most demanding BDE-scaled group of accelerograms (orange), and relevant biaxial moment safe domains (blue) in the presence of the LFT top addition.

By way of example of these results, the M_Y–M_X biaxial moment interaction curves plotted in **Fig. 5** for the two most stressed columns in as-built conditions are duplicated in **Fig. 12** in the presence of the upper addition. The peak response values are about 26% (column O-1) and 28% (column O-2) higher than the corresponding values computed in current state. Consequently, the borders of the safe domains are exceeded by about 60% and 75% for columns O-1 and O-2, respectively.

At the SDE, the maximum *IDR* values are equal to 0.13% in *X* (30% higher than in current state) and 0.46% in *Y* (15% higher), still below the IO-related limit of 0.5%. At the BDE, the inter-storey drifts increase by about 20%, reaching 1.41% in the O longitudinal alignment on the first storey, and slightly exceeding 1% on the I and M alignments of the same storey. A maximum *IDR* value of 0.77% is found on the O alignment of the ground storey, assessing severe damage conditions also for the infills belonging to this level.

The total estimated "turnkey cost" of the architectural addition amounts to € 1,700,000 Euros, corresponding to approximately 3,400 Euros/m^2.

5 Light-frame top addition including dissipative braces

As mentioned in the Introduction, the dissipative bracing solution adopted for the LFT top addition, hereafter named DB-LFT design configuration, is based on the incorporation of small-sized pressurized fluid viscous spring-dampers at the tip of the supporting inverse-chevron steel trusses. The mechanical behaviour of these devices, whose working principle is based on the flow of a pressurized highly viscous fluid through a thin annular space between piston head and tank casing [28], is reproduced by the following damping, F_d, and non-linear elastic, F_{ne}, force components:

$$F_d(t) = c \cdot sgn\left[\dot{x}(t)\right]\left|x(t)\right|^{\gamma} \tag{10}$$

$$F_{ne}(t) = k_2 x(t) + \frac{(k_1 - k_2)\,x(t)}{\left[1 + \left|\frac{k_1 x(t)}{F_0}\right|^5\right]^{1/5}} \tag{11}$$

where: t = time variable; c = damping coefficient; $sgn(\cdot)$ = signum function; $\dot{x}(t)$ = velocity; $|\cdot|$ = absolute value; γ = fractional exponent, ranging from 0.1 to 0.2; F_0 = static pre-load; k_1, k_2 = stiffness of the response branches situated below and beyond F_0; and $x(t)$ = axial displacement.

The basic design objective of incorporating the DB system only into the LFT structure consisted in nearly annulling, or at least mostly mitigating, the increase in member stress states and inter-storey drifts induced by the top addition. At the same time, by limiting the incorporation of the system into the perimeter frames and a few internal frames, the architectural impact on the interiors of the new apartments could be minimized.

The nominal energy dissipation capacity, E_n, of the spring-dampers, which represents their explicit design parameter, was estimated with the energy-based procedure formulated in [29]. This consists in assigning the set of PFV devices to be installed on a given (*j-th*) storey, in this case represented by the top addition, the energy capability, E_{Dj}, of dissipating a prefixed fraction, β_j, of the maximum seismic input energy, E_{Ij}, computed by the numerical model of the structure on the same storey. E_{Ij} and E_{Dj} are expressed as follows:

$$E_{Ij} = \int_0^t m_j \ddot{d}_{tj} \dot{d}_g \, dt \tag{12}$$

where: m_j = mass and $\ddot{d}_{tj}$ = absolute acceleration of the *j-th* storey, and $\dot{d}_g$ = ground velocity;

$$E_{Dj} = \int_0^t c_j sgn\left(\dot{d}_j\right)\left|\dot{d}_j\right|\gamma \dot{d}_j \, dt \tag{13}$$

where: c_j = total damping coefficient of the set of PFV spring-dampers of the *j-th* storey, given by the sum of the damping coefficients of each device placed on that storey; $\dot{d}_j$ = velocity of the *j-th* storey.

By computing the input energy, given by the only contribution of the modal energy, for the top storey, a value of about 120 kJ resulted. Then, according to the criteria discussed in [21] and by considering the specific characteristics and design objectives of this installation (limited to one building level only, and particularly the top storey, where the maximum seismic response accelerations are reached), it was assumed to assign the DB system nearly 100% of the input energy, i.e. to put β_j as equal to 1, and thus $E_{Dj} = E_{Ij} = 120$ kJ. Based on this assumption, one of the smallest types of PFV spring-dampers currently in production was tentatively adopted first, hereafter referred to as SD1-type, with the following mechanical properties, taken from the manufacturer's catalogue [30]: $E_n = 7$ kJ, $c = 9.9$ kN·(s/mm)$^{\gamma}$, with $\gamma = 0.15$, $F_0 = 17$ kN, $k_2 = 1.74$ kN/mm, maximum response force $F_{max} = 150$ kN, stroke $x_{str} = \pm 30$ mm, diameter of the external casing 90 mm, length (stroke excluded) 210 mm. By referring to the E_n value of 7 kJ, 12 pairs of SD1-type devices, and thus 24 spring-dampers, were adopted, the total maximum energy dissipation capacity of which is equal to: $E_{n,t} = 24\ E_n = 168$ kJ, which covers with reasonable safety margins the tentatively computed maximum energy dissipation demand $E_{Dj} = 120$ kJ. It can be noted that the PFV spring-damper model immediately smaller than the selected SD1-type has a E_n value of 4.8 kJ, which provides a $E_{n,t}$ total capacity slightly smaller than $E_{Dj} = 120$ kJ. Eight spring-damper pairs were installed in transversal direction, and namely in spans G-2/G-3, G-4/G-5, I-2/I-3, I-4/I-5, M-2/M-3, M-4/M-5, O-2/O-3, O-4/O-5, and four pairs in longitudinal direction, in spans G-2/I-2, G-5/I-5, M-2/O-2, M-5/O-5. These positions are visualized in **Fig. 13** by red and green rectangles, respectively, along with the drawings of one of the four identical transversal panels and one of the eight identical longitudinal panels.

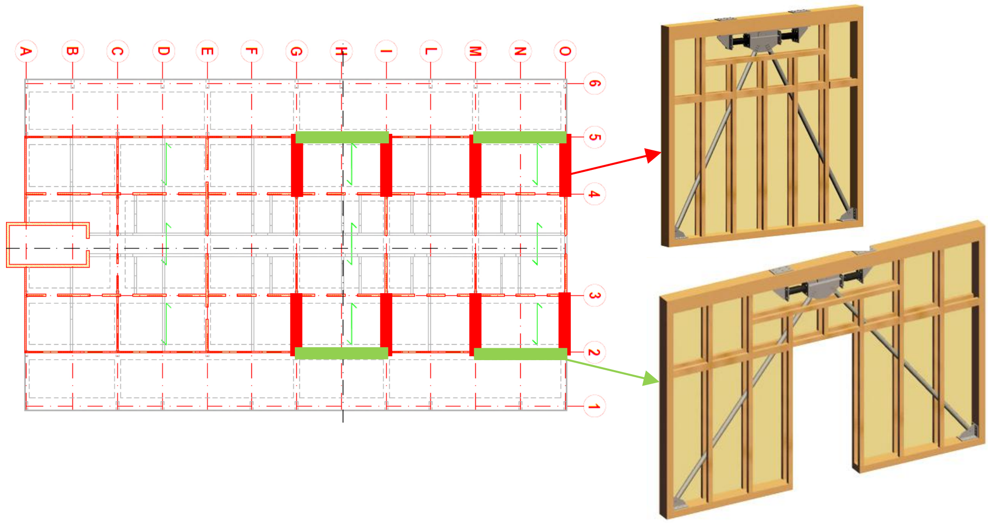

Fig. 13. LFT structure spans incorporating the DB system.

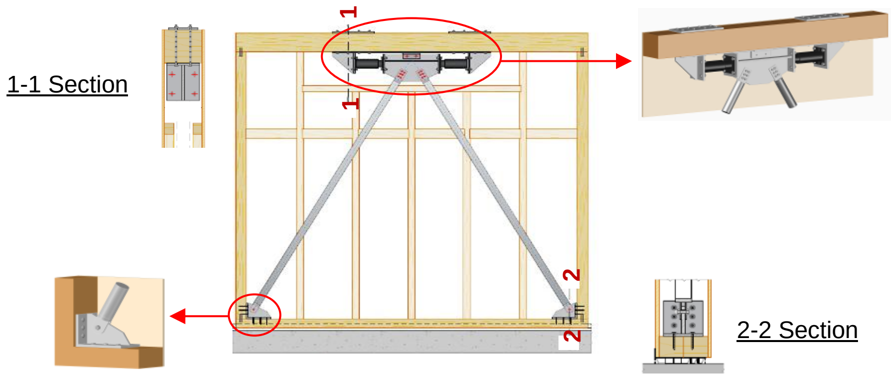

Fig. 14. Installation details of the DB system into the LFT panels.

The installation details of the system are presented in **Fig. 14**, consistent with the general mounting scheme adopted in several early [29] through recent [31] applications of this technology. A circular tubular section with 88.9 mm diameter and 3.2 mm thickness is adopted for the steel braces, M12 bolts for their connections to the central steel plate to which the spring-dampers are joined, and screws with diameter of 9 mm and length of 100 mm for the connection of the base steel plates to the bottom plate–to–stud joint. The relatively small sizes of braces, bolts and screws are a consequence of the F_{max} = 150 kN maximum response force design value transmitted by the spring-dampers to the braces and relevant connections.

Views of the finite element model of the top-added structure incorporating the dissipative braces are shown in **Fig. 15**. Due to a very low increase in lateral stiffness produced by the DB system, determined by the in-series connection of the diagonal trusses and PFV devices and the low axial stiffness of the elastic component of the latter, the modal parameters remain virtually unchanged as compared to the conventional LFT solution. Indeed, the first mixed mode has a period of 0.695 s and EMMs of 60.6% along *Y* and 21.5% around *Z*, and the first translational mode in *X* has a period of 0.276 s and EMM of 82.9%. Furthermore, the same numbers of modes are needed to activate a SMM greater than 85% in *Y* (4) and *Z* (5); in *X*, one more mode is needed (24). At the SDE, all structural members pass the stress state checks; the maximum *IDR* values are equal to 0.14% in *X* and 0.43% in *Y*, i.e. practically halfway between the values calculated in current state and the ones of the conventional top addition solution.

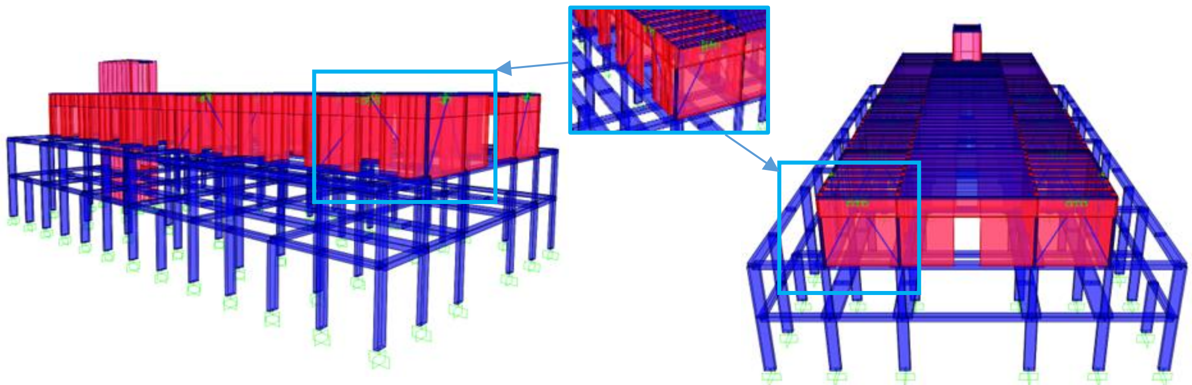

Fig. 15. Views of the finite element model of the structure including the DB-LFT top addition.

As compared to the latter, at the BDE the percentage of columns in unsafe conditions drops to 33% on the ground storey and 24% on the first storey, and the percentage of beams drops to 20% (ground) and 13% (first). These percentage values are also lower than the ones in current state, except for four first storey columns, which pass to unsafe conditions, although with demand/capacity ratios only slightly greater than 1.

Fig. 16 shows the M_Y–M_X biaxial moment interaction curves for the same columns which **Fig. 6** and **Fig. 12** refer to. The maximum values are about 10% higher than in as-built conditions for both columns, and about 14% (O-1) and 15% (O-2) smaller than for the LFT conventional solution.

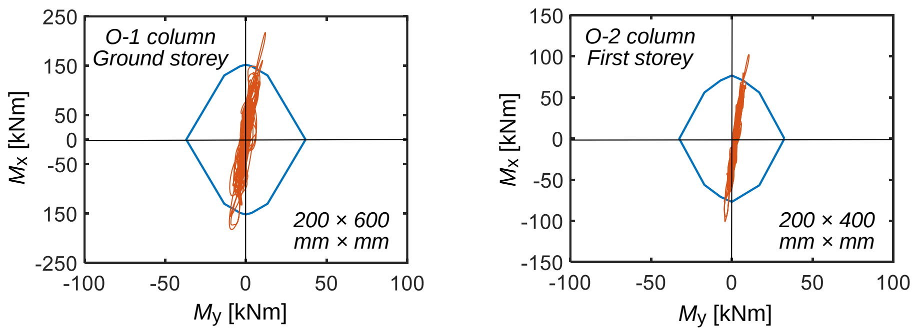

Fig. 16. M_y-M_x biaxial moment interaction curves for ground storey O-1 column and first storey O-2 column obtained from the most demanding BDE-scaled group of accelerograms (orange), and relevant biaxial moment safe domains (blue) in the presence of the DB-LFT top addition.

Fig. 17 duplicates the images in **Fig. 5** and **Fig. 11**, highlighting the reduced number of unsafe columns and beams as compared to the LFT top addition without dissipative braces.

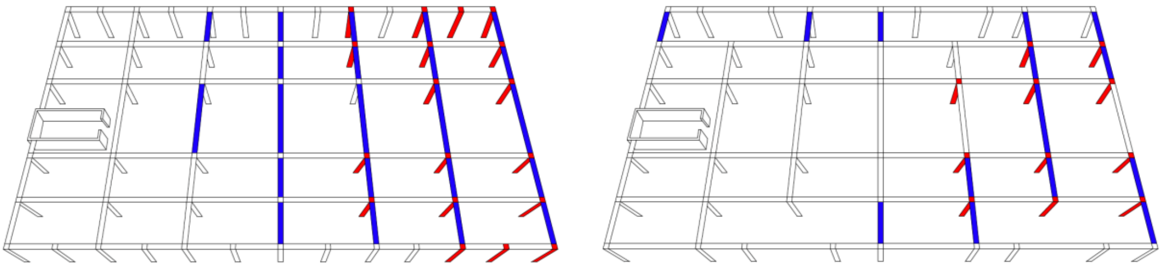

Fig. 17. Location of the structural elements in unsafe conditions in the presence of the DB-LFT the top addition (left: ground storey, right: first storey).

Benefits are also observed as compared to the current state (33% against 35% of ground storey columns in unsafe conditions, and 13% against 18% of first storey beams, with equal 20% of ground storey beams), with the only exception of the first storey columns (24% against 15%). The peak inter-storey drifts decrease from 1.42% to 1.23% on the first storey, and from 0.77% to 0.67% on the ground storey as compared to the conventional LFT design, with a very slight increase (equal to 0.04% for both drifts) as compared to the current state.

By way of example of the dissipative bracing system performance, **Fig. 18** shows the response cycles of the spring-damper pairs installed in the O-2/O-3 and M-2/O-2 spans obtained from the most demanding BDE-scaled group of accelerograms. These graphs highlight that the devices positioned in the stiffer *X* direction achieve maximum displacements of 3.5 mm, equal to 40% of the ones reached by the dampers installed along *Y* (8.9 mm). Therefore, thanks to their early activation, also the former devices provide an appreciable contribution to the seismic protection of both the superstructure and the underlying structure. This also occurs for the dampers installed in spans G-2/G-3, G-4/G-5, G-2/I-2 and G-5/I-5, subject to lower torsion response effects in plan, reaching displacements greater than 6 mm in *Y* and 3 mm in *X*.

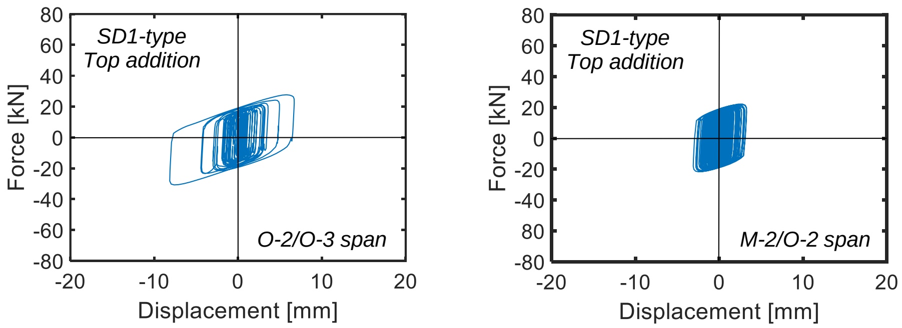

Fig. 18. Response cycles of the pairs of SD1-type PFV spring-dampers installed in the O-2/O-3 and M-2/O-2 spans of the DB-LFT top addition obtained from the most demanding BDE-scaled group of accelerograms.

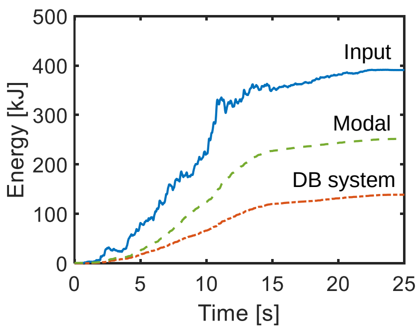

Fig. 19. Energy time-histories in DB-LFT configuration obtained from the most demanding BDE-scaled group of accelerograms.

The energy response time-histories of the building obtained from the same input accelerograms which **Fig. 18** is referred to are plotted in **Fig. 19**. As shown by these graphs, the energy dissipated by the DB system is equal to about 138 kJ, i.e. equal to 35% of total input energy, and 15% greater than the above-mentioned value E_{Dj} =120 kJ assumed as tentative energy demand in the design of the DB system.

The reduced seismic response of the top structure as compared to the conventional LFT solution confirms that no intervention on the foundation is needed.

The estimated additional cost for the incorporation of the DB system, given by the sum of the cost of manufacturing and installation of the PFV spring-dampers and the diagonal braces and relevant connection plates (no other cost being necessary), is equal to 65,000 Euros, i.e. less than 4% of the total construction cost of the upper addition mentioned in Section 4.2.

The design choices of including the DB system only into the twelve selected spans of the LFT addition and using only SD1-type spring-dampers were finally reassessed by increasing the number of spans and/or hypothesizing PFV devices with higher energy dissipation capacities. Both checks showed negligible benefits on the seismic performance of both the LFT and the RC structures. Therefore, the design assumptions define a "best choice" solution from a structural point of view, in addition to minimizing architectural impact, use of materials and costs.

6 Extension of the dissipative braces to the RC structure

The improved seismic performance of the building achieved thanks to the DB-LFT design solution as compared to the conventional LFT one, with only slightly higher construction costs, led to extend the DB system also to some spans of the RC structure, with the aim of attaining its seismic retrofit. For this third intervention, denoted as DB-LFT+RC in the following, the three central spans of the O transversal alignment, i.e. spans O-2/O-3, O-3/O-4 and O-4/O-5, were tentatively selected for the installation of the additional dissipative braces on both the ground and first storeys. This choice allows to limit the intervention only to the exterior of the building, as well as to prevent any obstruction of the side façade, which features only a small window in the wider central span, not crossed by the diagonal trusses. At the same time, from a structural point of view, as the O alignment is subjected to the greatest drifts in *Y*, the dissipative capacity of the PVF spring-dampers and their constraining action against seismic torsional effects in plan are maximized.

The basic design objective of the DB system extension consisted in bringing all structural members to safe conditions, except for a few beams (6% on the ground storey, and 4% on the first storey) that meet the stress state checks under gravitational loads with small margins. This suggested to slightly strengthen them, regardless of the results of the seismic assessment analyses.

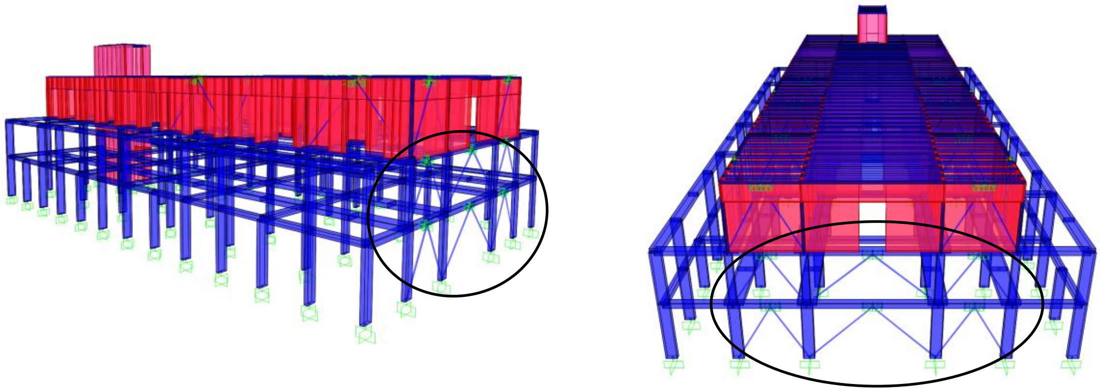

Fig. 20. Views of the finite element model of the structure including the DB system (highlighted by a black ellipse) also into the RC frame.

The *c* coefficients of the additional spring-dampers were estimated using the same procedure adopted for the devices installed in the superstructure. In this case, according to the pre-sizing criteria recalled in Section 5, and specialized in [29] to RC frame structures, 80% percentile fraction (i.e. β_{j} = 0.8) of the maximum seismic input energy on the ground and first storeys was assigned to the spring-dampers to be installed within them. As the modal energy computed at the BDE for the two storeys in DB-LFT configuration was equal to 180 kJ, the following damping energy demand was tentatively assigned to the DB system: (180 × 0.8) = 144 kJ. Based on this preliminary estimate, and in order to restrict the installation of the DB system exclusively to the three spans mentioned above, a PFV spring-damper with immediately greater dissipation capacities than the SD1-type devices installed in the LFT structure, as drawn from the manufacturer's catalogue, was adopted. This second dissipator, named SD2-type, has the following mechanical properties [30]: c = 14.16 kN·(s/mm)$^{\gamma}$, with γ = 0.15, F_0 = 28 kN, k_2 = 2.1 kN/mm, E_n = 14 kJ, F_{max} = 230 kN, x_{str} = ±40 mm, diameter of the external casing 110 mm, length (stroke excluded) 257 mm. Views of the finite element model including the additional dissipative braces are represented in **Fig. 20**.

The technical installation details of the DB system are similar to the ones adopted for the top addition. It is noted that, on all storeys, adhesives are not required for installation, as the steel plates of the bracing system are connected to the LFT studs and plates only with screws and to the RC columns and beams only with steel anchors; thus, in the event of a future dismantling of the DB system, no residues or traces would remain on the structures. The small stiffening produced by the incorporation of the DB system in the RC structure results in a fundamental period in *Y* of 0.656 s, i.e. 5.6% lower than for the DB-LFT configuration, with EMMs of 61.6% along *Y* and 20.6% around *Z*, whereas the period of the first translational mode in *X* remains the same (0.276 s). Five modes are needed to activate a SMM greater than 85% in *Y*, 24 in *X* and 6 in *Z*.

At the SDE, maximum *IDR* values of 0.06% in *X* and 0.16% in *Y* are computed on the first storey, i.e. less than half the corresponding values in DB-LFT configuration, and equal to 0.05% in *X* (coinciding with the DB-LFT value) and 0.03% in *Y* (four times lower) on the top addition. At the BDE, the peak drifts drop from 0.39% to 0.23% (first storey) in *X* and from 1.23% to 0.64% in *Y*, on the first storey; and from 0.35% to 0.19% in *Y* on the top addition, with an unchanged value of 0.14% in *X*. Therefore, only the peak first storey values in *Y* assess repairable damage conditions of infills at the BDE, whereas all remaining *IDR* values denote a completely undamaged response.

All columns pass to safe conditions at the BDE. This is highlighted by the M_Y–M_X curves in **Fig. 21**, still referred to the ground storey column O-1 and the first storey column O-2, which are completely constrained into relevant safe domains. Concerning beams, as five of them (three on the ground storey and two on the first storey) meet the stress state checks under static loads with narrow margins. As a consequence, they result in slightly unsafe conditions under seismic action scaled at the BDE intensity also in DB-LFT+RC configuration, thus requiring only limited strengthening measures. To minimize the architectural impact and sustainability, the interventions could consist in bonding single sheets of carbon fiber reinforced (CFR) fabrics to their end zones.

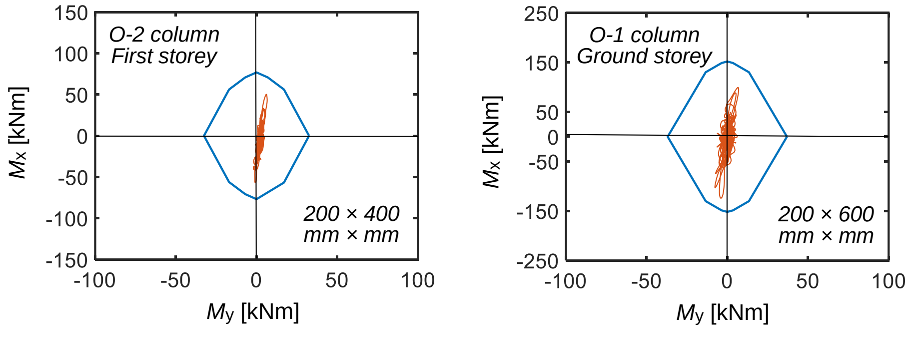

Fig. 21. M_y-M_x biaxial moment interaction curves for ground storey O-1 column and first storey O-2 column obtained from the most demanding BDE-scaled group of accelerograms (orange), and relevant biaxial moment safe domains (blue) in DB-LFT+RC configuration.

Fig. 22 shows the response cycles of the SD2-type spring-damper pairs installed in the O-2/O-3 spans on the ground and first storeys of the RC structure obtained from the most demanding BDE-scaled group of accelerograms. The maximum displacements reached by the devices on the two storeys (10.6 mm—ground, 17.5 mm—first) are in the same proportion as the corresponding peak *IDR* values in current state. This is consistent with the objective of significantly reducing drifts and torsional effects in plan, while keeping the modal displacement profile of the frame structure substantially unchanged.

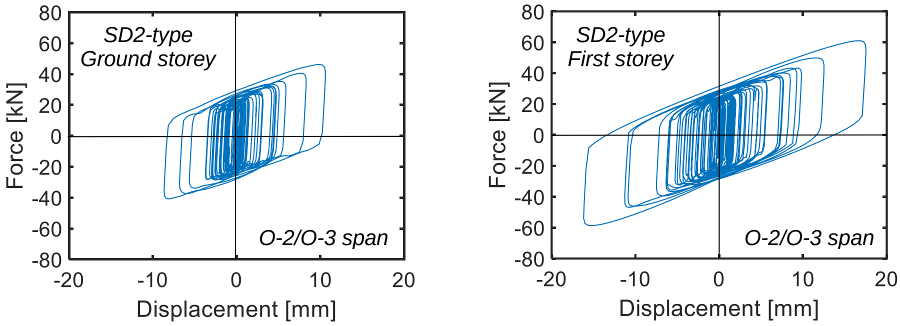

Fig. 22. Response cycles of the pairs of SD2-type PFV spring-dampers installed in the O-2/O-3 spans of the ground and first storeys of the RC structure in DB-LFT+RC configuration obtained from the most demanding BDE-scaled group of accelerograms.

The response cycles of the spring-dampers installed in the O-2/O-3 and M-2/O-2 spans of the top addition are plotted in **Fig. 23**. By comparing these graphs with the corresponding ones shown in **Fig. 18** for the DB-LFT solution, a reduction of 25% is observed in the maximum displacements of the dampers of span O-2/O-3 (6.7 mm against 8.9 mm), and almost identical values for the devices of span M-2/O-2 (3.3 mm against 3.5 mm). Therefore, the incorporation of the DB system in the RC structure produces a benefit also in the response of the overlying spans of the LFT structure, which justifies to keep in the latter the spring-dampers adopted in DB-LFT configuration, without the need to increase their size to improve further the building performance.

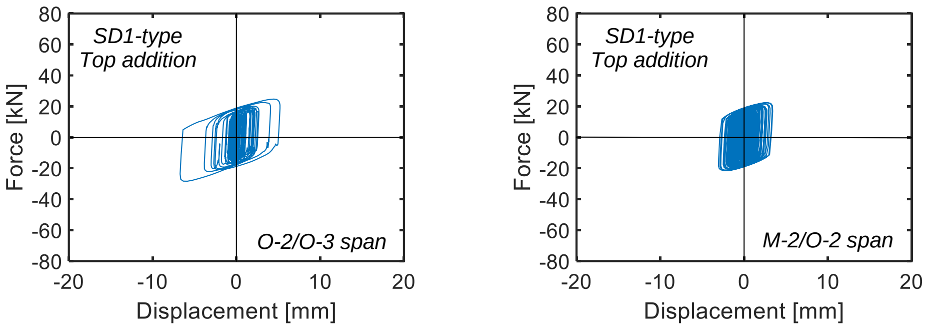

Fig. 23. Response cycles of the pairs of PFV spring-dampers installed in the O-2/O-3 and M-2/O-2 spans of the top addition in DB-LFT+RC configuration obtained from the most demanding BDE-scaled group of accelerograms.

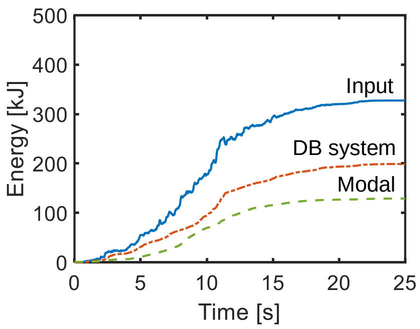

Fig. 24. Energy time-histories in DB-LFT+RC configuration obtained from the most demanding BDE-scaled group of accelerograms.

The energy response time-histories obtained in DB-LFT+RC configuration, graphed in **Fig. 24**, show that in this case the DB system dissipates approximately 60% of the total input energy. By comparing these curves with the corresponding ones in **Fig. 19**, it is noted that the almost halving of drifts in the RC structure induced by the response of the dissipative braces included in it leads to almost halving modal energy too, which falls from about 265 kJ to 129 kJ. The total energy dissipated by the

DB system rises from 138 kJ to 199 kJ. The latter value is given by the sum of the energy dissipated by the SD1-type spring-dampers installed in the top addition, equal to 69 kJ, and the energy dissipated by the SD2-type devices incorporated in the first and second storeys, equal to 130 kJ. This value is 10% smaller than the above-mentioned value of 144 kJ tentatively estimated, with a reasonable prudential margin, in the pre-sizing design phase of the SD2-type devices.

Thanks to the low stiffening effects of the DB system, the corresponding small increase in the axial force of the ground storey columns does not require any interventions on the foundation slab, like for the conventional LFT and DB-LFT design solutions.

The cost of the retrofit intervention on the RC structure, demolition and reconstruction of the external layers of the infills of the six spans involved plus all finishes, amounts to about 120,000 Euros, corresponding to 80 Euros/m^2 of the total covered area of the existing building. The cost of conventional retrofit strategies that could be adopted as an alternative, such as wrapping by FRP fabrics of the 34 columns and 39 beams in unsafe conditions in the presence of the LFT top addition, would be more than double, amounting to approximately 280,000 Euros. This possible alternative solution would also have a significant architectural impact on the apartments and would cause a temporary interruption in their use, resulting in additional costs and a reduced sustainability of the interventions. Other traditional retrofit strategies, consisting in the incorporation of non-dissipative braces or RC shear walls within the building, would further increase both costs (over 400,000 Euros) and architectural, functional and sustainability impact.

Table 1. Summary of structural performance and cost of the three types of interventions

		Current state	LFT	DB-LFT	DB-LFT+RC
Fundamental period	[s]	0.568	0.697	0.695	0.656
Maximum IDR	[%]	1.19	1.41	1.23	0.64
Unsafe RC columns	[%]	26	36	29	0
Unsafe RC beams	[%]	19	18	17	5
Intervention cost	[€]	-	1,700,000	1,765,000 (+65,000)	1,885,000 (+120,000)

Table 2. Maximum absolute displacement and dissipated energy of the PVF spring-dampers

Span	DB-LFT		DB-LFT+RC	
	d_{xmax} [mm]	E_d [kJ]	x_{max} [mm]	E_d [kJ]
Top addition				
G-2/G-3	7	9	4	3
G-2/I-2	5	11	5	11
G-4/G-5	7	9	4	3
G-5/I-5	5	11	4	10
I-2/I-3	8	11	5	3
I-4/I-5	8	10	5	3
M-2/M-3	9	12	5	3
M-2/O-2	5	11	4	11
M-4/M-5	10	13	6	4
M-5/O-5	5	11	4	10
O-2/O-3	11	15	7	4
O-4/O-5	11	15	7	4
First storey				
O-2/O-3	-	-	17	29
O-3/O-4	-	-	19	31
O-4/O-5	-	-	17	29
Ground storey				
O-2/O-3	-	-	11	13
O-3/O-4	-	-	17	15
O-4/O-5	-	-	11	13

A final summary of the main structural characteristics and performance parameters obtained for the four different configurations of the case study building at the BDE, as well as of the cost estimated for each intervention, is offered in **Table 1**. Furthermore, in **Table 2** the response of each pair of PFV spring-dampers (denoted with the corresponding span of installation) is listed in terms of maximum absolute displacement, x_{max}, and dissipated energy, E_d, for the DB-LFT and DB-LFT+RC design solutions.

7 Conclusions

The study presented in this article aimed at offering new contributions on the use of light-frame timber structures for building top additions and the incorporation of dissipative systems into these structures. On one hand, a design and performance assessment analysis of "platform-frame"-type LFT top additions was developed, providing suggestions in terms of seismic conception and finite element modelling, and evaluating the consequences of the additions on the response of the underlying buildings. On the other hand, the incorporation of a special DB system equipped with small-sized pressurized fluid viscous spring-dampers into the LFT panels was proposed and discussed. The possibility of extending the PFV-equipped DB system to the existing structure was also investigated, with a view to achieving its seismic retrofit.

Detailed remarks derived from the results of the study carried out by referring to a representative real building with RC structure are summarized below.

– The equivalent shell finite elements used to simulate the response of the LFT structure—whose mechanical properties were evaluated by the criteria revised here from scientific and technical literature—allowed to easily carry out the computational analyses, and are suggested for use in similar analyses by scholars and professionals.

– Due to its intrinsic lightness, the conventional LFT structure adopted as first design hypothesis for the architectural addition produced a moderate growth in the seismic demand on the underlying RC structure. This was assessed at the SDE, with maximum drift values still below the 0.5% IO-related normative drift limit; and at the BDE, with the percentage of columns in unsafe conditions rising from 35% to 41% on the ground storey, and from 15% to 30% on the first storey, and a virtually unchanged number of beams failing the stress state checks.

– The incorporation of the PFV-equipped DB system into the timber structure allowed to meet the basic design objective of almost annulling the increase in demand caused by the upper addition, thus leaving the seismic performance of the RC structure virtually unchanged as compared to its current state. Indeed, the percentage of beams in unsafe conditions remains unchanged on the ground storey and falls from 20% to 13% on the first storey; at the same time, the percentage of unsafe columns decreases from 35% to 33% on the ground storey. The only exception is represented by four first storey columns that pass to unsafe conditions, though with only a slight increase in their demand/capacity ratios (just under 1 in current state, and no greater than 1.1 in the presence of the top addition including the DB system).

– Thanks to the high specific damping capacity of the PFV dissipators, this design objective was achieved by limiting the incorporation of the DB system only in eight perimeter frames and four internal frames. Furthermore, the compact sizes of the devices and their supporting steel trusses allow them to be hidden behind the OSB sheathing panels of the LFT structure.

– The basic design objective of extending the DB system to the RC structure, i.e. bringing to safe conditions all structural members, except for a few beams meeting the stress state checks under gravitational loads with small margins, was reached by limiting the extension to only the three central spans of the side façade of the building (8% of the total of transversal spans). This allowed to prevent any architectural intrusion in the interiors of the building, and thus any interruption in its use.

– The additional cost for the incorporation of the DB system in the superelevation is less than 4% of its total construction cost.

– At the same time, the estimated cost of the retrofit intervention of the RC structure amounts to 120,000 Euros, corresponding to 80 Euros/m^2 of the total covered area of the existing building. This cost is significantly lower than the one of conventional retrofit strategies that could be adopted as an alternative, such as wrapping of the RC members by FRP fabrics, which amounts to approximately 280,000 Euros, or the incorporation of non-dissipative braces or RC shear walls, exceeding 400,000

Euros.

– In terms of sustainability, in the event of a hypothetical future dismantling, all three interventions are substantially recyclable, as they are made entirely of wood and, for the two solutions including dissipative braces, of steel elements, connected to the LFT members only with screws and to the RC columns and beams only with steel anchors.

Although these results are limited to a single case study, they provide a positive initial indication of the feasibility of incorporating the PFV-equipped DB system—so far applied to various types of heavy-frame RC and steel structures—also into the seismic design of LFT top additions of buildings.

Funding Statement

This study was supported by the Italian Department of Civil Protection within the ReLUIS-DPC Project 2024-2026 – Work Package 12: Steel, timber and composite civil and industrial constructions [grant nr. 1100004434, 10.13039/50].

CRediT authorship contribution statement

Arianna Straulino: Methodology, Investigation, Software, Formal analysis, Data curation, Validation, Visualization, Writing – original draft. **Stefano Sorace**: Conceptualization, Methodology, Supervision, Validation, Writing – original draft, Writing – review & editing, Funding acquisition. **Naisa Hoxha**: Investigation, Software, Formal analysis, Data curation, Visualization. **Gloria Terenzi**: Conceptualization, Methodology, Validation, Visualization.

Conflicts of Interest

The authors declare that they have no conflicts of interest to report regarding the present study.

Data Availability Statement

Some or all data, models, or codes that support the findings of this study are available from the corresponding author upon request.

References

[1] Ugalde D, Almazán JL, Santa María H et al. Seismic protection technologies for timber structures: a review. European Journal of Wood and Wood Products 2019; 77: 173–194. https://doi.org/10.1007/s00107-019-01389-9.

[2] Filiatrault A. Analytical predictions of the seismic response of friction damped timber shear walls. Earthquake Engineering and Structural Dynamics 1990; 19: 259–273. https://doi.org/10.1002/eqe.4290190209.

[3] Dinehart DW, Shenton HW, Elliott TE. The dynamic response of wood-frame shear walls with viscoelastic dampers. Earthquake Spectra 1999; 15: 67–86. https://doi.org/10.1193/1.1586029.

[4] Higgins C. Hysteretic dampers for wood frame shear walls. In proceedings of 2001 Structures congress and exposition, ASCE. Washington D.C., USA, 1-9. doi: 10.1061/40558(2001)180.

[5] Rigo P., Polastri A., Mazelli A., Bedon C., Casagrande D. Experimental and numerical analysis on Light-Frame Timber shear-walls coupled with self-centering steel cables. Construction and Building Materials, 2025; 504: 144393. https://doi.org/10.1016/j.conbuildmat.2025.144393.

[6] Symans MD, Cofer WF, Du Y, Fridley KJ. Evaluation of fluid dampers for seismic energy dissipation of woodframe structures. CUREE - Caltech Woodframe Project Report W-20. Stanford Digital Repository, 2002. Available at: http://purl.stanford.edu/dy867jw4956.

[7] Dutil DA, Symans MD. Experimental investigation of seismic behavior of light-framed wood shear walls with supplemental energy dissipation, in: 13th World Conference on earthquake engineering. Vancouver, Canada, August 1-6, 2004, Paper No. 3421, p 15.

[8] Shinde JK, Symans MD, Liu H, van de Lindt JW. Seismic performance assessment of woodframed structures with energy dissipation systems, in: 18th Conference on Analysis and Computation held in Conjunction with ASCE/SEI Structures Congress. Vancouver, Canada, April 24-26, 2008, p 9. https://doi.org/10.1061/4000(1315)27.

[9] Shao X, van de Lindt JW, Bahmani P et al. Real-time hybrid simulation of a multi-story wood shear wall with first-story experimental substructure incorporating a rate-dependent seismic energy dissipation device.

Smart Structures and Systems 2014; 14: 1031–1054. https://doi.org/10.12989/SSS.2014.14.6.1031.
[10] Bahmani P, van de Lindt JW, Gershfeld M et al. Experimental seismic behavior of a full-scale four-story soft-story wood-frame building with retrofits. I: building design, retrofit methodology, and numerical validation. ASCE Journal of Structural Engineering 2016; 142(4): 4. https://doi.org/10.1061/(ASCE)ST.1943-541X.0001207.
[11] Tian J, Symans MD, Pang W et al. Application of energy dissipation devices for seismic protection of soft-story wood-frame buildings in accordance with FEMA Guidelines. ASCE Journal of Structural Engineering 2016; 142(4): 14. https://doi.org/10.1061/(ASCE)ST.1943-541X.0001269.
[12] Van de Lindt JW, Bahmani P, Mochizuki G et al (2016) Experimental seismic behavior of a full-scale four-story soft-story woodframe building with retrofits. II: shake table test results. ASCE Journal of Structural Engineering 2016; 142(4): 5. https://doi.org/10.1061/(ASCE)ST.1943-541X.0001206.
[13] López-Almansa F, Segués E, Cantalapiedra IR. A new steel framing system for seismic protection of timber platform frame buildings. Implementation with hysteretic energy dissipators. Earthquake Engineering and Structural Dynamics 2015; 44: 1181–1202. https://doi.org/10.1002/eqe.2507.
[14] Casagrande D., Setti A., Polastri A. Structural behaviour of light-frame timber shear-walls with diagonal board sheathing. Construction and Building Materials 2024; 416: 135077. https://doi.org/10.1016/j.conbuildmat.2024.135077.
[15] Mohammadi H., Min Sun, Malek S. Effect of hold-down systems on the lateral performance of mid-rise light-frame wood shear walls under earthquakes – A comprehensive numerical study. Structures 2025; 76(10): 109050. https://doi.org/10.1016/j.istruc.2025.109050.
[16] Qiang R., Zhou L.,Chun Ni, Huang D. Seismic performance of high-capacity light wood frame shear walls with three rows of nails. Engineering Structures 2022; 268: 114767. https://doi.org/10.1016/j.engstruct.2022.114767.
[17] Qiang R., Zhou L.,Chun Ni, Huang D. Reversed cyclic testing of high-capacity light wood frame shear walls with two and three rows of nails. Engineering Structures 2024; 304: 117582. https://doi.org/10.1016/j.engstruct.2024. 117582.
[18] CSI, SAP2000NL. Theoretical and user's manual. Release 26.01, Computers & Structures Inc., Berkley, CA, USA, 2026.
[19] Ministerial Decree 17 January 2018. Update of Technical Standards for constructions, Italian Ministry of Infrastructure and Transport, Rome, Italy, GU no. 42–2018 (in Italian).
[20] Gelfi P. SIMQKE_GR. Univesity of Brescia, Italy. 2009. https://gelfi.unibs.it/software/simqke/simqke_gr.htm.
[21] Circular 21 January 2019 no. 7. Instructions for the application of the Update of Technical Standards for Constructions. Italian Ministry of Infrastructure and Transport, Rome, Italy, 2019, G.U. no. 35–2019 (in Italian).
[22] Sorace S, Costoli I, Terenzi G. Seismic assessment and dissipative bracing retrofit-based protection of infills and partitions in RC structures. Engineering Structures 2023; 281: 115781. https://dx.doi.org/10.1016/j.engstruct.2023.115781.
[23] CNR-DT 206-R1. Instructions for design, execution and control of timber structures, CNR – Italian National Council of Research, Rome, Italy, 2018 (in Italian).
[24] Rothoblaas SRL. Systems for walls, floors and buildings – Alu Start. https://www.rothoblaas.com/products/fastening/brackets-and-plates/angle-brackets-and-plates-for-buildings/alu-start/, 2026 (accessed January 24, 2026).
[25] Casagrande D, Rossi S, Sartori T, Tomasi R. Proposal of an analytical procedure and a simplified numerical model for elastic response of single-storey timber shear walls. Construction and Building Materials 2016; 102: 1101–1112. http://dx.doi.org/10.1016/j.conbuildmat.2014.12.114.
[26] Lauriola M. P. Timber constructions. Internal note, University of Florence, Florence, Italy (in Italian). https://files.supersite.aruba.it/media/17043_6c39be83e92a78ad94ce9bc64ab4cf196dc21b70.pdf/o/dispense_lauriola-31.pdf, 2025.
[27] Premrov M, Šilih EK. Numerical Study on In-Plane Behaviour of Light Timber-Framed Wall Elements Under a Horizontal Load Impact. Buildings 2025; 15: 778. https://doi.org/10.3390/buildings15050778.
[28] Sorace S, Terenzi G. Non-linear dynamic modelling and design procedure of FV spring-dampers for base isolation. Engineering Structures 2001; 23(12): 1556–1567. https://doi.org/10.1016/S0141-0296(01)00063-3.
[29] Sorace S, Terenzi G. Seismic protection of frame structures by fluid viscous damped braces. ASCE Journal of Structural Engineering 2008; 134(1): 45–55. https://doi.org/10.1061/(ASCE)0733-9445(2008)134:1(45).
[30] Dyna Shock System, Products & services. http://www.dynashocksystem.com/, 2026 (accessed 13 March 2026).
[31] Sorace S, Bidoli N, Terenzi G. Glazed-level dissipative brace incorporation in a gym building. Structures 2024; 68: 107184. https://doi.org/10.1016/j.istruc.2024.107184.